15th World Congress on Computational Mechanics (WCCM-XV)
8th Asian Pacific Congress on Computational Mechanics (APCOM-VIII)
Virtual Congress: 31 July – 5 August 2022
S. Koshizuka (Ed.)

# A TWO-DIMENSIONAL BIO-CHEMO-HYDRO-MECHANICAL MODEL FOR IN-SITU STABILIZATION OF SOILS USING BIOCHEMICAL PROCESSES

**PAVAN KUMAR BHUKYA**[1] **AND DALI NAIDU ARNEPALLI**[2]

[1] Indian Institute of Technology Madras
Chennai, India
ce19d200@smail.iitm.ac.in

[2] Indian Institute of Technology Madras
Chennai, India
arnepalli@iitm.ac.in

**Key words:** MICP, Finite Element Method, BCHM Model, Return Mapping Algorithm

**Abstract.** *Ground improvement techniques involving chemical additives are often energy-intensive and unsustainable due to the environmental distress caused by them. Sustainable biocementation processes such as microbially induced calcite precipitation (MICP) can overcome the drawbacks of traditional ground improvement techniques. Capturing the underlying coupled mechanisms in the biocementation process requires the knowledge of diverse fields of bio-chemo-hydro-mechanics. Modeling such a complex phenomenon is imperative for the successful implementation of the stabilisation technique in the field. The existing coupled models on biocementation are chiefly intended to validate the observed behavior of laboratory-scale biocemented specimens. This scenario demands the need to develop a coupled bio-chemo-hydro-mechanical (BCHM) model for field simulations. The BCHM model was developed with finite element and backward Euler finite difference approximations in space and time. The Galerkin weak formulations are derived for the mass balance equations of the coupled model. The advective-governed transport phenomena are accommodated with the Petrov-Galerkin formulation. An overall kinetically controlled reactive model is implemented to reproduce the urea hydrolysis and associated chemical kinetics. The reduced permeability of the biocemented soil is accounted in terms of its effective porosity, using the modified Kozeny-Carman equation. The fixed-point iteration scheme is implemented for bio-chemo-hydraulics to deal with the nonlinearity in the balance equations. The mechanical constitutive response of biocemented soil is simulated using a micromechanical framework. The von Mises and Drucker-Prager plasticity models were adopted for the biocement and soil particle phases, respectively. The integration of plasticity models was carried out using a return mapping algorithm. The Newton Raphson scheme is considered for the finite element implementation of elastoplastic models. The fully coupled nonlinear finite element problem is solved in a staggered approach using the developed MATLAB routine. The contour plots of biomass and chemical concentrations and precipitated calcite content are generated. The considered elastoplastic model predicted improvement in mechanical strength of biocemented specimen. A complete bio-chemo-hydro-mechanical behavior of the two-dimensional geometry is captured.*

## 1 INTRODUCTION

Ground stabilization is essential for the strength improvement of weak geomaterials. However, conventional chemical strengthening techniques introduce harmful chemical agents into the subsurface and contaminate natural resources. Over the past decade, the Microbially Induced Calcite Precipitation (MICP) process demonstrated effectiveness in improving the engineering behavior of geomaterials. Additionally, the MICP process is environmentally friendly compared to traditional chemical stabilization techniques [1]. The MICP process utilizes urease enzyme-producing bacteria to hydrolyze the urea ($CO(NH_2)_2$) and generates ammonium ion ($NH_4{}^+$). The hydrolyzed urea increases the pH of the chemical reaction and drives the reaction towards calcite ($CaCO_3$) precipitation in the presence of a calcium source ($Ca^{2+}$) [Eq.1]. The most common urease-producing bacterium is *Sporosarcina Pasteurii*.

$$CO(NH_2)_2 + 2\,H_2O + Ca^{2+} \xrightarrow{\text{urease}} 2\,NH_4{}^+ + CaCO_3 \tag{1}$$

Following the enzymatic reaction, the precipitated calcite binds the soil particles together and increases the strength and stiffness of the virgin soil. In addition to strength enhancement of geomaterials, the biocementation process has the potential to address many field problems, including erosion control, leak mitigation from $CO_2$ sequestrated aquifers, and slope stabilization [1]. Even so, the field trials of the MICP process are still limited [2]. The uncertainties involved in the MICP process are the prime factors for the unpredictable field complications. Therefore, the MICP process needs to be modeled to improve the reliability of successful field implementation. Nevertheless, capturing the underlying coupled mechanisms in the MICP process requires diverse fields, namely, bio-chemo-hydro-mechanics (BCHM). Past coupled models on biocementation are mathematically complex and computationally intense [2, 3]. Consequently, developing a robust yet simplified BCHM coupled model for multiphysics simulations is necessary.

To perform field simulations, the numerical model must be verified against laboratory simulations a priori. Hence, a BCHM model is developed in the current study to understand the biocementation process at a laboratory scale. The present work implements the principles of bio-chemo-hydraulics (BCH) based on the mathematical framework proposed by Wang and Nackenhorst [1]. In addition, the mechanical response of biocemented soil is predicted using a micromechanical constitutive framework proposed by Abdulla and Kiousis [4]. The advantage of the micromechanical approach lies within the modified hardening rules, which include cementation effects. In an effort to integrate the constitutive framework, the closest point projection algorithm employed by Spiezia [5] is utilized. Furthermore, the accuracy of the stress integration algorithm is verified by plotting Iso-error maps. Finally, the BCHM simulations are performed on a two-dimensional geometry with a prime objective of acquiring strength gain upon bicementation.

## 2 MATHEMATICAL FRAMEWORK

### 2.1 Bio-chemo-hydraulics (BCH)

The porous domain in the BCH model comprises soil solid and fluid phases. The soil mass having the porosity of $\phi$ is assumed to be saturated with a single fluid phase (water). Besides, the chemical species (urea, $NH_4^+$, and $Ca^{2+}$) are considered to exist only in the suspended form. But in contrast, the bacterial species lies in both suspended and attached forms. Furthermore, the soil solid phase acquires the mass influx from suspended bacteria and calcium carbonate precipitates. However, modeling transport processes of a suspended species at a continuum scale requires mass balance. Therefore, the transport of

the suspended species ($i$) in the porous media is given using a generalized mass balance equation [Eq.2]. The relevant suspended species under transport are suspended bacteria (bacl), urea (u), calcium ion ($Ca^{2+}$) and ammonium ion ($NH_4^+$). Additionally, the changes in the transport process of each suspended species is effected by the source/sink term ($\Omega_i$). In the present case, it is the function of the reaction rate of the biochemical reaction.

$$\phi\frac{\partial C_i}{\partial t} = \nabla.(\phi D.\nabla C_i) - q.\nabla C_i + \Omega_i \tag{2}$$

where, D is the diffusion dispersion tensor, q is the Darcy's flow velocity ($\phi v$), and $C_i$ is the concentration of suspended species $i$. It is comprehensible that the transport equation [Eq.2] captures the advective-diffusive-reactive transport processes in the soil domain. The advective transport of a species in the liquid phase requires the determination of Darcy's flow velocity (q). Moreover, due to the presence of biochemical species in the liquid phase, the fluid is considered as compressible. Hence, a macroscopic mass balance equation is adopted for a compressible fluid flow in the reactive soil media [Eq.3]. The advective flow in the current study is governed by Darcy's law, which estimates the advective flow velocity (q) using the pressure changes in soil media [Eq.4]. Additionally, the dispersion phenomenon is accommodated along with diffusion to include the effects of tortuous flow paths [Eq.5]. Nevertheless, the advective velocity plays a major role in deciding the stability of the finite element solution. Hence, advective dominated flows need special attention of introducing the Petrov-Galerkin formulation. On the other hand, diffusion-driven flows give smooth finite element solutions and are stable with conventional Bubnov-Galerkin formulation.

The reactive kinetics during the transport of species is simplified concerning Michaelis-Menten kinetics [Eq.6]. Consequently, the biochemical reactions with the maximum urease constant ($u_{sp}$) follow an overall kinetically controlled reaction [1]. The reaction rate depends on both total bacterial concentration ($C_{bact}$) and urea concentration ($C_u$). Considering the same reaction rate, the chemical species source terms follow the form of $\phi\tau_i k_{rea}$. The individual reaction coefficient of each chemical species is $\tau_{urea}$ = -1, $\tau_{Ca^{2+}}$ = -1 and $\tau_{NH_4^+}$ = 2.

Besides, first-order bacterial kinetics is incorporated to capture bacterial attachment and decay. However, the growth of bacteria is neglected as the bacteria at peak growth will be chosen for injection. Also, the attached bacterial concentration is directly dependent on the amount of suspended bacteria in the fluid phase. Hence, the corresponding mass transport equation for the attached bacteria (bacs) follows the proportionality [Eq.7]. Further, the calcium carbonate concentration at any given time is a function of reaction rate ($k_{rea}$) [Eq.8].

$$\beta_l\rho_l\phi\frac{\partial P_l}{\partial t} = \nabla.\frac{K\rho_l}{\mu_l}(\nabla P_l - \rho_l g) - m^u\phi k_{rea} - m^{Ca^{2+}}\phi k_{rea} + 2m^{NH_4^+}\phi k_{rea} \tag{3}$$

$$q = -\frac{K}{\mu_l}.(\nabla P_l - \rho_l g) \tag{4}$$

$$D = D_m + (\alpha_L - \alpha_T)\frac{v\otimes v}{|v|} + \alpha_T|v|I \tag{5}$$

$$k_{rea} = u_{sp}C_{bact}\frac{C_u}{K_m + C_u}\exp\left(\frac{-t}{t_d}\right) \tag{6}$$

$$\frac{\partial C_{bacs}}{\partial t} = k_{att}C_{bacl} - k_d C_{bacl} \tag{7}$$

$$\frac{\partial C_{CaCO_3}}{\partial t} = k_{rea} \tag{8}$$

where $\beta_l$ is the compressibility of fluid, $\rho_l$ is the variable liquid density, K is the permeability of the soil, $\mu_l$ is the viscosity of the fluid, g is the gravitation constant, $m^{urea}$, $m^{NH_4^+}$, $m^{Ca^{2+}}$ are the molar masses of urea, ammonium ion and calcium ion, $D_m$ is the molecular diffusion tensor, the $\alpha_L$ and $\alpha_T$ are longitudinal and transverse dispersion coefficients representing the mechanical dispersion, $K_m$ is the half-saturation constant, t is the time, and $t_d$ is the time constant that controls the maximum reaction rate.

The transport characteristics of the biochemical species are most affected by the permeability of the soil. Therefore, a modified Kozeny-Carman (KC) relation is adopted in the current study to capture permeability changes during cementation. The permeability changes of the soil domain are accounted for in terms of its effective porosity changes [6]. Therefore the considered permeability relation incorporates clogging effects representing a realistic behavior. The unspecified details implemented in the current BCH model can be found at Wang and Nackenhorst [1].

### 2.2 Mechanics (M)

In addition to flow and transport processes, the deformation characteristics of the biocemented specimen are essential. Hence, the mechanical response of MICP-treated soil is modelled using a micromechanical constitutive model [4]. The cement bonds precipitated due to the BCH processes improves the strength of the virgin soil mass. The additional bonding effects due to cementation are required in material modeling to capture the strength gain. Accordingly, von Mises and Drucker-Prager models are included to capture soil and cement phase mechanical responses. The momentum balance equation and constitutive relations are acquired for the finite element implementation of the mechanics module [Eq.9-12].

$$\nabla.\sigma + b = 0 \tag{9}$$

$$\sigma = \mathbb{D}\varepsilon \tag{10}$$

$$\mathbb{D} = \mathbb{D}_s + n_c\mathbb{D}_c + \sigma_c S^T + (1-n_c)\mathbb{D}_w - \mathbf{u}S^T \tag{11}$$

$$\varepsilon = \frac{1}{2}\left(\nabla u_d + \nabla {u_d}^T\right) \tag{12}$$

where, $\sigma$ is the total stress tensor of cemented soil phase, b is the body load, $\mathbb{D}$ is the constitutive tensor of soil-cement mixture, $n_c$ is the volumetric cement content, $\varepsilon$ is the total strain tensor, and $u_d$ is the total displacement. The additional information about mechanical constitutive model implemented in the current model is available at Abdulla and Kiousis [4].

### 2.3 Numerical strategy

The governing differential equations of the overall BCHM model are summarized in the above subsections. The Galerkin weak formulations are derived for each governing equation for finite element

implementation. Additionally, the advection-dominated flow is accompanied by the Upwind Petrov-Galerkin approach with artificial diffusion [7]. The time discretization is performed using an implicit Euler finite difference approximation. The system of linear and nonlinear equations of the BCH model are solved using the fixed-point iteration method. In contrast, the current model's mechanics module (M) employs the Newton-Raphson algorithm and line search algorithm using an elastic tangent stiffness tensor. The closest point projection method is incorporated for stress integration of constitutive model using the methodology implemented by Spiezia [5].

The coupled BCHM model is simulated in a staggered approach. Initially, the numerical algorithm solves hydraulics to determine Darcy's flow velocity (q). Darcy's velocity is included in suspended species mass transport weak formulation with a nodal averaged value. In addition, if the flow is advectively dominated at any given time step, the Petrov-Galerkin weighting function replaces the Bubnov-Galerkin weighting function. Furthermore, the chemical injection phase explicitly updates the porosity, permeability, and reaction rate at each step. Finally, with the information on precipitated calcium carbonate content, the mechanics module (M) is solved to evaluate deformations in biocemented soil mass while subjecting it to gradual shearing.

## 3 MODEL DEVELOPMENT

A two dimensional domain is considered for the current study with the dimensions of 0.125m $\times$ 0.5m [Fig.1(a)]. The domain is discretized with three noded triangular elements at a mesh size of 0.05m. The discretized geometry is subjected to bacterial, chemical, and mechanical loads. The problem is solved in three consecutive phases [Fig.1(a)]. At first, the bacterial injection phase (BI) is simulated with an injection rate of $8.3\text{x}10^{-5}$ m/s for 1 hr. duration. The flow and transport characteristics of bacteria are obtained simultaneously using [Eq.3,4]. This is followed by a retention phase (RT) for 8 hrs. duration subjecting the top and bottom surfaces of the domain to atmospheric pressure while allowing the bacteria to attach. The chemical injection phase (CI) is simulated for 4 hrs. duration at the rate of $1.8\text{x}10^{-5}$ m/s. The CI phase initiates the enzymatic reaction and precipitates calcite [Eq.1]. The improved mechanical response of the biocemented specimen is captured using a micromechanical elastoplastic constitutive model [4]. For the current study, the boundary conditions considered for the BCH model are adopted from Test 3B of Wang and Nackenhorst [1]. However, mechanical boundary conditions are adopted considering a bi-axial test case with plane strain condition. The complete boundary exposure during BCHM model is shown in [Fig.1(a)].

The subjected loading conditions of the domain (bacterial, chemical, and mechanical) are represented in the form of a timeline [Fig.1(b)]. The bacterial injection is performed at an optical density of 0.43 $OD_{600}$. This is followed by the retention phase maintaining zero flux conditions. Later, chemicals are injected with the chemical concentrations of 50mM each. As the chemical injection induces calcite precipitation, it results in a proportional strength gain. Following that, the biocemented specimen is confined to 0.5MPa and subjected to shearing, upto the peak mechanical load of 2.5MPa [Fig.1(b)]. The input data adopted for the BCH model is included in Table 1. In addition, the mechanical model parameters considered are indicated in Table 2. The mechanical parameters are assumed based on the fact that the approximate cumulative w/w cementation content of the specimen achieved is 4% [Fig.2(b)].

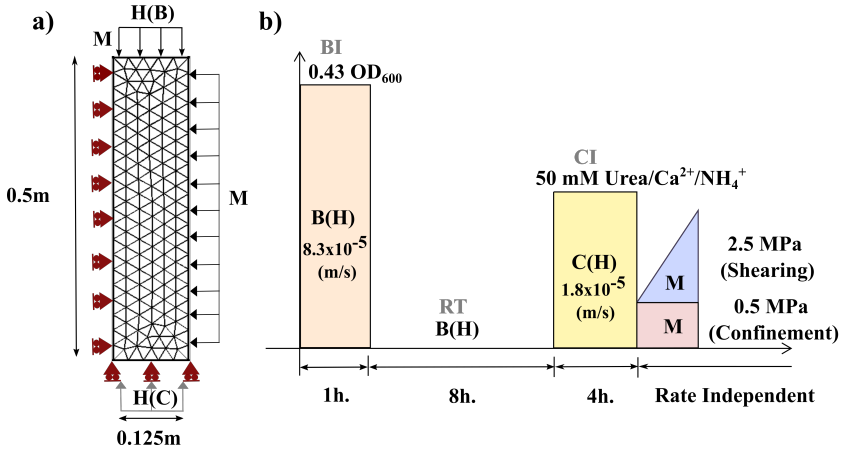


**Figure 1:** (a) Boundary conditions of the BCHM model (b) Timeline of injection/ loading conditions

**Table 1:** Bio-chemo-hydraulic parameters for the simulation [1]

| **Parameter** | **Value** |
|---|---|
| *Hydraulic parameters* | |
| Water density ($\rho_w$) | 1000 (kg·m$^{-3}$) |
| Liquid viscosity ($\mu_l$) | 0.001 (Pa·s) |
| Porosity ($\phi$) | 0.38 (-) |
| Hydraulic conductivity (k) | 2.4x10$^{-4}$ (m·s$^{-1}$) |
| Constant a | 0.33 (-) |
| Critical porosity ($\phi_c$) | 0.33 (-) |
| Bacterial injection rate ($q_b$) | 8.3x10$^{-5}$ (m·s$^{-1}$) |
| Chemical injection rate ($q_c$) | 1.8x10$^{-5}$ (m·s$^{-1}$) |
| Dispersion coefficient ($\alpha_L$,$\alpha_T$) | 0.005, 0 (m) |
| *Biological parameters* | |
| Maximum urease constant ($u_{sp}$) | 7x10$^{-2}$ (mol·m$^{-3}$·s$^{-1}$·OD$_{600}^{-1}$) |
| Time constant ($t_d$) | 288000 (s) |
| Decay rate ($k_d$) | 3.18x10$^{-7}$ (s$^{-1}$) |
| Attachment rate ($k_{att}$) | 1.2x10$^{-3}$ (s$^{-1}$) |
| *Chemical parameters* | |
| Half saturation constant ($K_m$) | 10 (mol·m$^{-3}$) |
| Molar mass ($m^{urea}$, $m^{Ca^{2+}}$, $m^{NH_4^+}$, $m^{CaCO_3}$) | 0.078, 0.04, 0.018, 0.1 (kg·mol$^{-1}$) |
| Calcite density ($\rho_c$) | 2710 (kg·m$^{-3}$) |
| Diffusion constant (D) | 2x10$^{-9}$ (m$^2$·s$^{-1}$) |

## 4 RESULTS AND DISCUSSION

The bio-chemo-hydro-mechanical response is obtained after simulating the BCHM model over the proposed timeline [Fig.2]. The simulation response indicated a change in attached bacterial concentrations between the BI and RT phases. The phenomenon of attachment is observed to progress after the end

of the BI phase [Fig.2(a)]. This increase specifies that the retention period plays a key role in deciding the bacterial concentration in the soil mass. Moreover, the bacterial concentration alters the kinetic rate of enzymatic reaction. In this scenario, the retention phase was more effective in enhancing the bacterial population. Also, the initiation of the CI phase begins the reactive transport leading to the precipitation of calcium carbonate. The simulations indicated that the calcium carbonate gravimetric content is higher at the height of 0.2m [Fig.2(b)]. The response is apparent as the chemical injection is performed from the bottom of the domain. Hence, higher precipitation is pronounced to occur in the middle zone of the soil domain. A similar response is observed in Wang and Nackenhorst [1].

**Table 2:** Mechanical parameters for the simulation [4]

| **Parameter** | **Value** |
|---|---|
| *Soil phase* | |
| Elastic modulus parameter ($K_m$) | 3.4 (MPa) |
| Elastic modulus exponent (n) | 0.51 (-) |
| Poisson's ratio ($\upsilon_s$) | 0.29 (-) |
| Initial hardening constant ($\alpha_{so}$) | 0.2 (-) |
| Ultimate hardening constant ($\alpha_{sult}$) | 0.323 (-) |
| Loading surface constant ($E_{sa}$) | 20 (-) |
| Initial dilation rate constant ($\beta_{so}$) | 0.16 (-) |
| Dilation rate parameter ($\beta_{sp}$) | 0.02 (-) |
| *Cement phase* | |
| Gravimetric percentage cementation ($\omega_c$) | 4% (-) |
| Elastic modulus (E) | 114.4 (MPa) |
| Poisson's ratio ($\upsilon_c$) | 0.2 (-) |
| Initial cement volumetric content ($n_{co}$) | 0.0194 (-) |
| Damage parameter ($\Theta$) | 5.2 (-) |
| Initial hardening constant ($\alpha_{co}$) | 8.5 (MPa) |
| Ultimate hardening constant ($\alpha_{cult}$) | 16.6 (MPa) |
| Loading surface constant ($E^{\alpha}$) | 103.4 (MPa) |
| Compression coefficient ($\beta_{c\beta}$) | 1.3 (-) |
| Ultimate value of $\beta_c$($\Delta_{c\beta}$) | 0.012 (-) |

Simultaneously, the permeability of the domain reduces during the chemical injection phase due to precipitation. During CI, the clogging phenomenon is directly related to the precipitated calcium carbonate content. This is captured in the model using a modified KC equation [6]. Also, as higher calcium carbonate is materialized at 0.2m height, the permeability is observed to be the lowest at that particular location [Fig.2(c)]. Furthermore, the deformation characteristics due to mechanical loading are observed by simulating the mechanics module assuming 4% cementation. The simulations indicated lower vertical displacements in biocemented specimen [Fig.2(d)]. Nonetheless, this is because cemented bonds also resist cemented soil deformations during mechanical loading, indicating the strength enhancement of untreated soil due to the biocementation process.

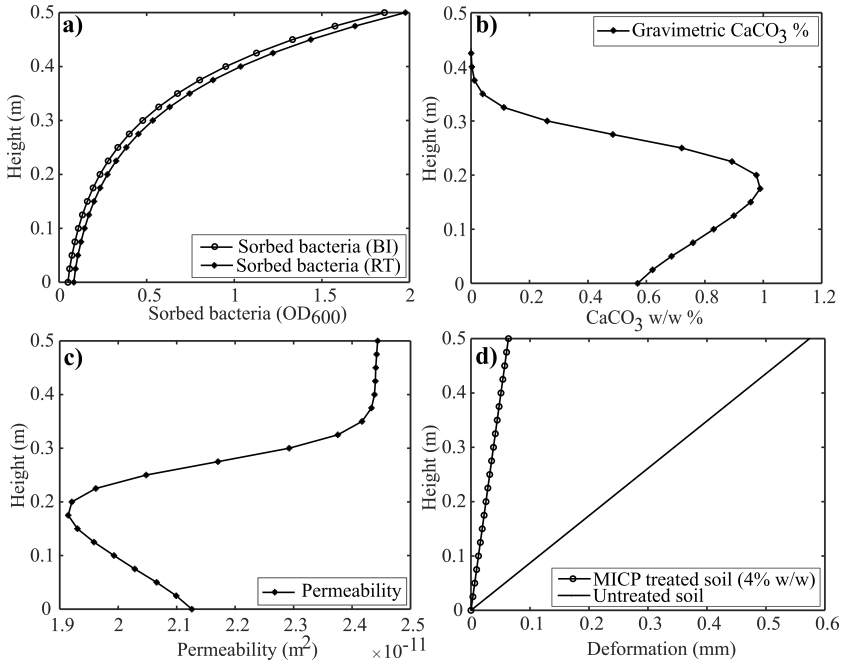


**Figure 2:** (a) Sorbed bacterial concentration ($OD_{600}$) at the end of bacterial injection (BI) and retention phase (RT) (b) Calcium carbonate gravimetric content (w/w %) at the end of chemical injection phase (CI) (c) Permeability of the domain ($m^2$) at the end of chemical injection (CI) (d) Deformation (mm) of uncemented and MICP treated domain

In regard to determine the accuracy of integration algorithms of constitutive models, Iso-error maps were generated at a strain level of 5% [8]. Because of the adopted micro-mechanical approach, the simulations demanded individual Iso-error maps for the soil and cement phase. Upon plotting, the maximum error observed in both the Iso-error maps for certain variable strain incremental rates is 0.1%. Implying that the implemented closest point return mapping algorithm is efficient in simulating bi-axial test condition.

## 5 CONCLUSIONS

The current work developed a numerical model to observe the bio-chemo-hydro-mechanical phenomenon during the biocementation process. A MATLAB routine has been developed using finite element and finite difference approximations in space and time. The closest point projection algorithm is adopted for the stress integration of von Mises and Drucker-Prager constitutive models. The Iso-error maps indicated an efficient return mapping algorithm with a maximum error of 0.1%. The numerical simulations implied an increased bacterial concentration at the end of the retention phase. Also, the carried-out simulations showed higher precipitation of calcium carbonate at the sample height of 0.2m. This suggests that the injection strategy is efficient in accumulating precipitation in the central region of the sample. Additionally, the permeability of the soil domain is reduced as the biocementation process progresses. Moreover, the biocemented specimen has shown minimal deformation under bi-axial shearing. Overall, the complete bio-chemo-hydro-mechanical response of a two-dimensional geometry is captured. The future scope of this work is to calibrate and implement the developed BCHM model

for field simulations. As the field implementation of the MICP process needs the hour, this model could indicate possible scenarios in the field.

## REFERENCES


[1] Wang, X. and Nackenhorst, U. A coupled bio-chemo-hydraulic model to predict porosity and permeability reduction during microbially induced calcite precipitation. *Adv. Water Resour.* (2020) **140**:103563.

[2] Cunningham, A.B., Class, H., Ebigbo, A., Gerlach, R., Phillips, A.J. and Hommel, J. Field-scale modeling of microbially induced calcite precipitation. *Comput. Geosci.* (2019) **23(2)**:399–414.

[3] Ebigbo, A., Phillips, A., Gerlach, R., Helmig, R., Cunningham, A.B., Class, H. and Spangler, L.H. Darcy–scale modeling of microbially induced carbonate mineral precipitation in sand columns.*Water Resour. Res.* (2012) **48(7)**.

[4] Abdulla, A.A. and Kiousis, P.D. Behavior of cemented sands–II. Modelling *Int. J. Numer. Anal. Methods Geomech.* (1997) **21(8)**:549–568.

[5] Spiezia, N. (2015). *Multiphase material modelling in finite deformations: theoretical aspects, numerical implementation and applications*. Ph.D. thesis, Department of Civil, Environmental and Architectural Engineering, University of Padua, Italy.

[6] Koponen, A., Kataja, M. and Timonen, J. Permeability and effective porosity of porous media. *Phys. Rev. E* (1997) **56(3)**:3319.

[7] Zienkiewicz, O.C., Taylor, R.L. and Nithiarasu, P. *The finite element method for fluid dynamics (Seventh Edition)*. Butterworth-Heinemann, (2013).

[8] Simo, J.C. and Hughes, T.J.R. *Computational inelasticity (Seventh Edition)*. Springer Science & Business Media, (2006).